Chapter 8

The Application of Electric Fields in Biology and Medicine

Francis X. Hart and John R. Palisano

Additional information is available at the end of the chapter

http://dx.doi.org/10.5772/intechopen.71683

Abstract

We discuss a wide range of applications of electric fields in biology and medicine. For example, physiological strength (<500 V/m) fields are used to improve the healing of wounds, the stimulation of neurons, and the positioning and activation of cells on scaffolds for tissue engineering purposes. The brief, strong pulses used in electroporation are used to improve the insertion of drugs into tumors and DNA into cell nuclei. The references direct readers to detailed reviews of these applications. The mechanism by which cells detect physiological strength fields is not well understood. We also describe a field-transduction mechanism that shares features common to the detection of fluid shear by cells. We then provide some experimental evidence that supports our model.

Keywords: electric field, wound healing, electroporation, galvanotaxis, glycocalyx

1. Introduction

The applications of electric fields in biology and medicine are many and varied. Physiological strength (~100 V/m), direct current (DC) electric fields are important in the development, maintenance and control of cells and tissues. Their role in wound healing, embryonic development, and tissue regeneration is described in detail in the reviews of Pullar [1], McCaig et al. [2], and Robinson and Messerli [3]. Endogenous DC electric fields are also important in embryonic patterning [4]. In tissue engineering cell proliferation on scaffolds can be controlled by the application of such fields [5]. At the tissue level electric fields are used for the measurement of body composition [6] and the promotion of wound healing [7]. An important new development has been the use of strong electric fields for drug delivery. Very high, pulsed fields can promote the passage of drugs through membranes [8] or the insertion of DNA into the nucleus for genetic engineering applications [9].

There are still unresolved questions regarding the mechanisms by which the fields achieve their effects. For physiological strength fields a wide variety of biochemical pathways within the cell following the initial detection of the field have been studied [10], but the initial transduction mechanism is not well understood. For high voltage, pulsed fields the details of membrane pore formation remain unclear.

Many papers have been published in this very broad area for many years. It is not possible to cover the many applications of electric fields in biology. We first describe some representative applications of electric fields in biology and medicine. Next we discuss mechanisms responsible for these effects and explore some remaining gaps in our understanding of these processes. References are provided to reviews so that readers who desire more detailed discussions of these applications can find them. For low field effects we also describe the experimental procedures used to accurately measure galvanotaxis, a process involved in several of the applications described here, and present some typical results.

2. The application of physiological strength DC and low frequency AC fields to cells and tissue

2.1. Wound healing

When tissue is damaged, an electric field is produced at the wound site. **Figure 1** illustrates how such fields are produced when epithelial tissue, such as skin, suffers a wound. The upper three layers of skin are the stratum corneum, the epidermis and the dermis. The figure illustrates three typical cells in a row in the epidermis. At the top or apical membrane of a cell sodium ions enter the cell via sodium-specific channels. At the bottom or basolateral membrane potassium ions leave the cell. These ionic transfers are associated with a biochemical reaction inside the cell involving ATP, which is a molecule with bonds for high-energy transfer in the cell. **Figure 1a** shows this transfer process prior to the development of a wound for the three cells. The cells are connected by tight junctions (TJ) that do not ordinarily permit the passage of charge. The flow of charge through the cell produced by this biochemical process has a current I associated with it. The layer above the apical membrane has given up positive charges to the sodium channels and thus has a relative negative charge. The layer below the basolateral membrane has acquired a relative positive charge. This charge imbalance is relieved by its return flow along a paracellular pathway i.e. through more distant junctions that are not so tightly bound. Because there is an electrical resistance R associated with this pathway, a potential difference $\Delta V = IR$ is produced across the entire epithelial layer. Depending on the particular tissue and pathway details, ΔV ranges between 15 to 60 mV [11].

Figure 1b shows the situation when the middle cell has been damaged. There is now an easy passage for the return flow to the apical layer. Positive charge from both directions will flow along the basolateral membrane layer toward the wound. There is thus an associated electric field, E, directed toward the wound from both sides. The field strength for this endogenous field is about 100–200 V/m at the wound site. For a more detailed explanation of the biochemical origin of the field see the review by Nuccitelli [11]. For examples of how widespread

http://dx.doi.org/10.5772/intechopen.71683

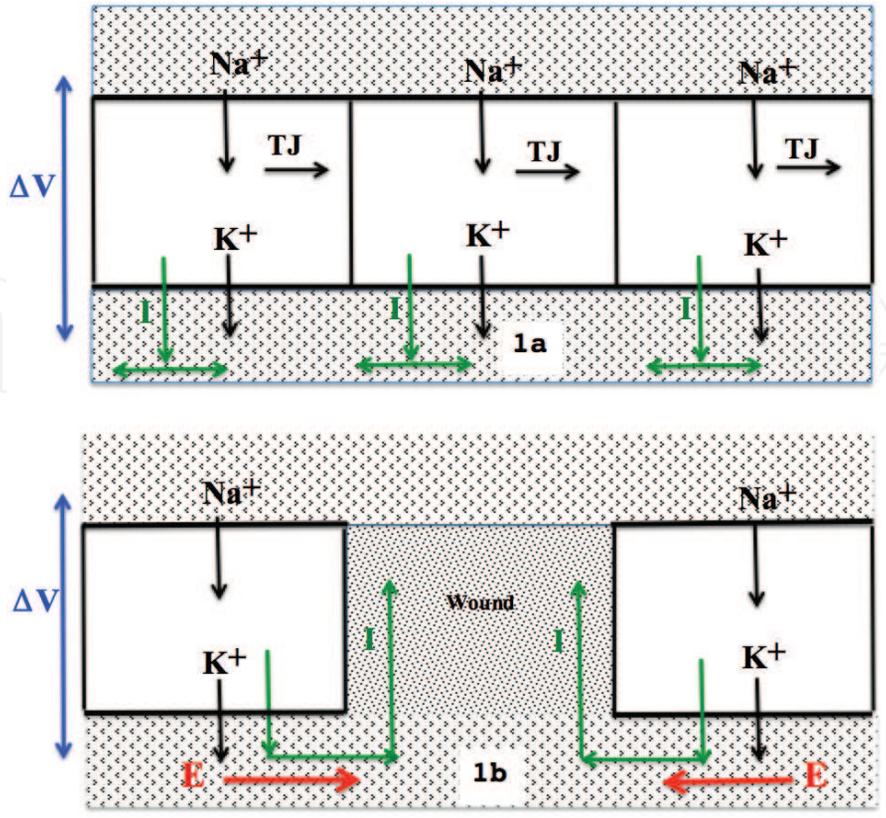

Figure 1. Schematic diagram of the electric field produced at a skin wound site.

wound-generated fields are in biological systems (e.g., plants), see the review by Robinson and Messerli [3].

Just as cells migrate in response to a chemical gradient (chemotaxis), most types of cell also migrate in response to an electric field (galvanotaxis or electrotaxis). In response to a nearby wound, cell types such as keratinocytes, fibroblasts, macrophages and lymphocytes migrate toward the wound under the guidance of the field [12, 13]. Most cells migrate in the direction of the field toward the negative pole. The situation is complicated, however. Macrophages move toward the positive pole although their precursors, monocytes, migrate toward the negative pole [14]. Moreover, when an endogenous field is not produced at the wound site, the wound does not heal properly. Application of an external electric field might then improve the healing of wounds that have not healed on their own by directing the migration of cells to the wound site and also by inducing those cells to produce biochemicals that promote healing [13]. For example, a negative electrode could be placed on the wound and one or more electrodes connected to a positive pole placed nearby. Kloth [12] has reviewed a number of clinical studies that have investigated whether the application of such fields improves the treatment of wounds compared to standard wound care. The applied fields in such studies are either constant direct current (DC) or pulsed direct current. Analyzing a wide variety of devices, Kloth [12] found that the most effective treatments used a current ranging between 250 and 500 μA. Some of these devices have been approved by regulatory agencies for wound healing in the EU and for antibacterial activity on wounds in the US.

2.2. Electrical stimulation of the nervous system

Pulsed and low-frequency alternating current (AC) fields, applied with either implanted or surface electrodes, are being used to either stimulate or suppress neural activity. In Deep Brain Stimulation (DBS) [15] electrodes can be surgically implanted into specific areas of the brain to apply pulse signals that suppress endogenous signals that produce Parkinson's disease tremors or epileptic seizures. The neurostimulator, connected to the electrodes is usually implanted under the collar bone. DBS is generally applied as a supplement to regular medications and only after the medications no longer provide relief of symptoms. Over time the electrodes can become coated and may need to be replaced.

Electrical stimulation (ES) [16] has been successfully used to restore muscular functionality in patients who have suffered a major spinal cord injury (SCI). Although the spinal cord has been damaged, the muscular systems that it ordinarily stimulates may remain undamaged. If electrical signals can be transmitted to those muscles, they may respond as usual. ES can be applied to the peripheral nervous system or directly to the spinal cord. For peripheral stimulation electrodes are preferably implanted into the tissue close to the nerves. Otherwise, surface electrodes are used. Bipolar pulses are used in order to prevent electrochemical damage to the tissue near the electrodes. Complex movements, such as grasping by the hands, require the stimulation by multiple nerves in a particular temporal pattern. For this reason the power supply must generate pre-programmed, separate signals to the individual neurons. For a detailed description of ES systems and their application in restoring functionality for standing, bladder control, pressure ulcer prevention and other conditions see the review by Ho et al. [16].

The spinal cord can generate its own complex neural stimulation patterns if it receives the proper electrical stimulation. SCI can damage the cord above the region where it ordinarily generates signals for standing and walking so that these activities cannot be performed. Rejc et al. [17] report that application of pulses from an array of electrodes inserted into the epidural spaces of the spinal cord allowed several paraplegic individuals to stand with minimal assistance. The pulse patterns must be tailored to the individual. Solopova et al. [18] used skin electrodes to apply biphasic rectangular pulses to the lower spines of children suffering from cerebral palsy. This treatment, combined with treadmill training, improved locomotor function compared to locomotor training only.

Transcutaneous Electrical Nerve Stimulation (TENS) is a treatment by which low frequency pulses are applied by skin electrodes to reduce pain. Although the electrodes are generally placed at the site of the pain (e.g., lower back), the primary effects appear to be due to stimulation of the central nervous system. The lower frequency (<10 Hz) pulses are applied with a relatively high intensity to produce non-painful motor contraction whereas the high frequency (>50 Hz) are applied with a relatively low intensity and do not produce contractions. Both types of stimulus activate opioid receptors in the spinal cord and brain that reduce pain, but the type of opioids produced differs for the two stimuli. For more details see the review by DeSantana et al. [19].

2.3. Induced electric fields and bone healing and brain stimulation

2.3.1. Changing magnetic fields produce electric fields

The electric fields just described are produced by an electrical potential difference that is generated by batteries or power supplies. The electric field lines flow from positive to negative charges. Such sources are well suited for surface applications such as wound healing, corneal repair or even brain and spinal stimulation with closely-separated, inserted electrodes. However, they are not suited for the broad application of electric fields to deeper tissue because of the tissue's electrical impedance. Another method for producing electric fields uses Faraday's Law that describes how a time-varying magnetic field produces an induced electric field with field lines that are closed loops. Magnetic fields penetrate tissue unimpeded so that significant induced fields can be produced well below the body surface.

Consider a spatially uniform magnetic field, B, that varies with time, t. Suppose that the field is applied perpendicular to the surface of a circular metallic disc. The electric field, E, induced at a distance r from the center of the disc is a circular loop of radius r with a magnitude

$$E(r) = \frac{r}{2}\frac{dB}{dt} \tag{1}$$

It should be noted that the same field would be produced even in the absence of the metal disc. The field itself is independent of the material. The induced electric current, however, does depend on the material through its conductivity. For systems more complicated than a circular disc the calculation of the induced field is complicated and requires numerical methods. For a simple example of a square dish with insulating inclusions (e.g., cells) see Hart et al. [20].

2.3.2. Two examples illustrate the clinical use of time varying magnetic fields

For many years electric fields have been used to promote the healing of bone fractures that have not responded to the usual treatments. Because the fractures are located deep within tissue, implanted electrodes are not generally used. There are, however, two other ways by which external delivery systems can produce the required internal fields. Consider, for example, a fractured tibia. Pad electrodes can be placed on either side of the patient's calf. A high frequency signal applied to these electrodes will be capacitively coupled to the internal tissues, including the fracture site, to produce an electric field there. Alternatively, a coil system could be wrapped around the calf. A time-varying current in the coils produces a time-varying magnetic field in the calf that generates, in turn, a pulsed electromagnetic field (PEMF) at the fracture site. The PEMF stimulates osteoblasts so that the bone grows and proliferates to heal the fracture. Two meta-analyses [21, 22] of clinical studies of electrically stimulated bone healing show some improvements in the patients, but more well-defined studies are needed.

In transcranial magnetic stimulation (TMS) coils of various designs are placed around a patient's head. As with the bone fracture treatment the coils produce a time-varying magnetic field that inductively generates an electric field at the desired site in the brain. The coil

system design is chosen to produce a localized electric field at the desired site in the brain. This method is used, for example, to treat depression or to assess whether a particular motor area of the brain is stimulating the associated muscle system properly. For more details and examples of biomagnetic stimulation, see the review by Ueno and Sekino [23]).

2.4. Electric fields for diagnostic purposes

The preceding sections have described how the application of electric fields to cells and tissue can produce beneficial effects in those targets. Electric fields, however, can also be applied to monitor the physiological state of tissues for diagnostic purposes. All materials, including tissue, have an associated resistance, R, and capacitance, C [24]. If an AC voltage is applied to tissue, current that depends on both R and C will flow through the tissue. Capacitances restrict the flow of low frequency current, but allow high frequency currents to pass. The value of C determines the transition frequency range for passage and blockage of the AC current. For tissues that frequency is around 100 kHz–1 MHz.

Figure 2 depicts the Fricke circuit model commonly used for tissue. Re and Ri represent, respectively, the resistances of the extracellular and intracellular resistances. Both resistances are determined primarily by water content. C represents the capacitance of the cell membrane. Low frequency currents are blocked by C from the cell interior and thus serve as a measure of extracellular water. C allows high frequency currents to enter the cell interior and thus measure the combination of Re and Ri. Use of two frequencies allows the separation of Re and Ri and thus the determination of intracellular and extracellular water content.

These principles can be used for the measurement of body composition [6]. In healthy individuals there is a well-defined relationship between total body fat-free mass and the total body water mass. Knowledge of the total body fat-free mass and the total body mass yields the body's fat mass and thus the percentage body fat. Depending on the positions of the electrodes, this method can be used for measurements on the whole body or on specific limbs. Determination of changes in the ratio of Re to Ri can yield information regarding the possibility of fluid leakage (edema) into a limb.

A different application of the Fricke model is useful in the monitoring of breathing. The air in the lungs does not permit the flow of current and can be modeled as a time-varying C. Measurement

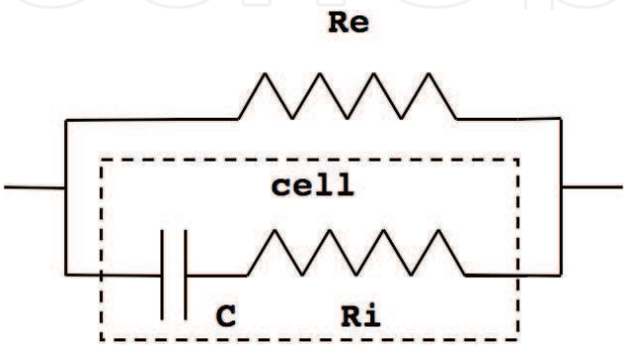

Figure 2. Fricke circuit model.

of the current over time yields the breathing rate and thus serves as a monitor of sleep apnea. How R and C vary over a wide range of frequencies could be used to differentiate healthy tissue from diseased tissue. The sensitivity of devices that identify breast tumors is not yet sufficient to receive governmental approval. For a detailed review of the various diagnostic uses of electric fields see the review by Hart [6].

2.5. Tissue engineering

The application of electric fields to cellular systems can produce a wide variety of physical effects in cells in addition to galvanotaxis. Such effects are described in detail in the CRC review monograph edited by Pullar [1]. This combination of electric field effects is proving useful in tissue engineering in which cells are deposited on a substrate (scaffold) and stimulated to grow into more complicated tissues. For example, the application of pulsed DC fields to cardiac myocytes cultured on a collagen sponge scaffold stimulated their alignment, coupling and synchronous contractions [25]. Such an assemblage would serve as a cardiac patch for heart attack victims. Pulsed fields promoted the outgrowth and orientation of neurites on a polypyrrole/collagen scaffold [26]. The goal of such research is to develop the ability to replace damaged nerves. A DC field applied to osteoblasts, the bone-forming cells, deposited on a titanium substrate increased their adhesion to the substrate and their proliferation [27]. The nature and structure of the substrate is important because it can provide mechanical stimulation that also affects cell behavior on a scaffold. Optimizing both contact guidance and the applied electric field produces results that are better than those obtained for either modality by itself for fibroblasts and cardiomyocytes [28] as well as corneal and lens epithelial cells [29].

Tissue engineering has typically used electric fields that were applied externally to the scaffold. Recently Arinzeh et al. [30] reported that the scaffold itself could provide the electric field used to control and stimulate the cells. They designed a scaffold that was part ceramic and part plastic. One of the plastic materials they used was piezoelectric; that is, it generated an electric field when mechanically stressed. With the proper piezoelectric-scaffold mechanical texturing, they were able to enhance axonal regeneration in neurites with the goal of promoting spinal cord repair. Moreover, using the proper piezoelectric materials and scaffold textures, they were able to induce stem cells to form either bone or cartilage. For a more detailed discussion of the use of electric fields in tissue engineering see the review by Hronik-Tupaj and Kaplan [31].

3. Cell dosimetry

In order to understand how cells produce the observed effects, it is first necessary to understand how the applied field is distributed within the cell as a function of time. Suppose that a spherical cell of radius R is placed within a culture medium far from parallel plate electrodes. At time t = 0 an electric field E is applied between the plates. The Fricke model shown in **Figure 2** can be used to understand the resulting charging of the cell membrane and induced transmembrane voltage TMVi. The cell behaves as a series RC circuit. When the field is applied, charge flows through the resistor to charge the capacitor. Once the capacitor is fully charged to establish TMVi, the

flow of charge through R ceases. The time constant for the process is τ. For times significantly less than τ there is significant charge flow and an associated electric field within the cell interior (cytoplasm). The voltage across the capacitor, the TMVi, gradually increases. For times significantly greater than τ charge flow has ceased and the associated electric field within the cytoplasm is negligible. The TMVi has reached its maximum value. Without the applied field, there is a natural transmembrane voltage, TMVo, that is produced by a system of ion pumps and channels in the membrane. TMVo is on the order of 70 mV for most cell types with the cell interior being more negative than the exterior. The total transmembrane voltage, TMVt, is then the sum of TMVo and TMVi. The transmembrane voltage varies with time [32] according to:

$$\mathrm{TMVt} = 1.5\mathrm{ER}\cos\Theta\left(1-\exp\left(-t/t\right)\right)+\mathrm{TMVo} \tag{2}$$

where Θ is the angle between the electric field and the normal to the cell surface. The 1.5 factor is related to the spherical shape of the cell and has higher values for more asymmetrically shaped cells. For irregularly shaped cells numerical modeling is required, as discussed in Section 6.

Figure 3 is a stylized diagram that illustrates a cell placed in an initially uniform electric field, Eo. When the field is first applied (t < <t), charge has not had sufficient time to flow to charge the cell membrane and there is a significant field inside the cell. After the field has been applied for a long time (t> > τ), the membrane is fully charged and the field in the cytoplasm is negligible. For typical cells τ is on the order of 1 microsecond. TMVi can be quickly estimated for an applied field of 100 V/m. The diameter of a small cell is on the order of 10 μm so that the potential difference across the cell is on the order of 1 mV. At equilibrium there is negligible potential difference throughout the cell interior. The 1 mV is shared by the membrane at its ends to give an

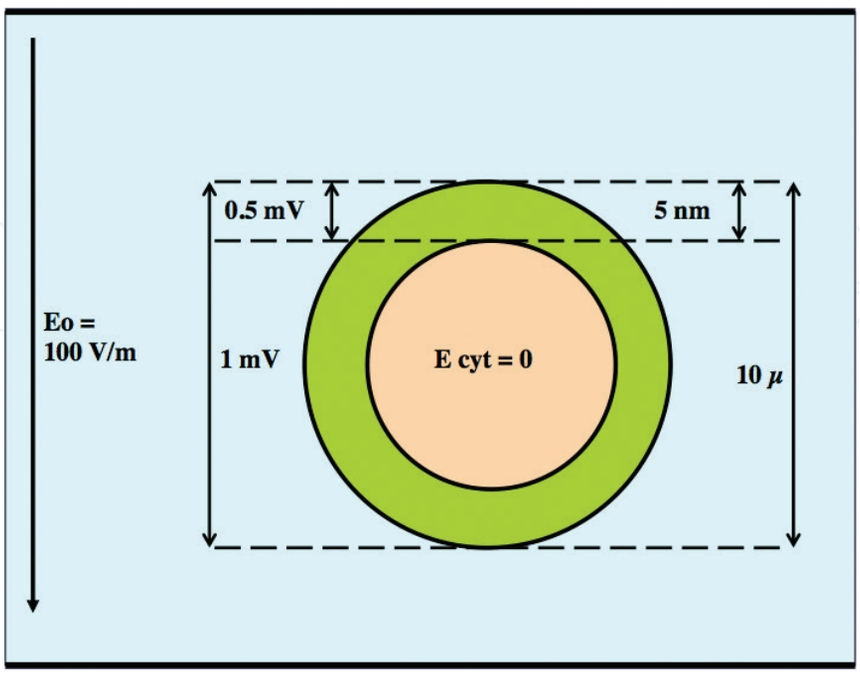

Figure 3. Dependence of the transmembrane voltage on the applied field.

estimated TMVi of 0.5 mV. The sphericity of the cell adds an additional factor of 1.5 to yield an actual TMVi of 0.75 mV. Note that this value is much less than TMVo. For a cell with a diameter of 50 mm the TMVi would be 3.75 mV, still small compared to the TMVo. For an applied field of 10 kV/m TMVi would be 75 mV for the 10 μm diameter cell and 375 mV for a 50 μm diameter cell. In these cases TMVi is comparable to or greater than Vo, respectively.

4. Electroporation

4.1. Basic principles

The applications described to this point are for applied fields of physiological strength; that is, less than about 300 V/m. The frequencies of these fields are also less than 1 MHz with corresponding time scales greater than 1 microsecond. As noted above, for such time scales the resulting cytoplasmic electric field is negligible, so any direct interaction must take place at the cell surface. In this section we discuss applications produced by fields that are on the order of 10 kV/m or greater with component frequencies often greater than 1 MHz. Such fields are strong enough to permeabilize the cell membrane; that is, to permit the passage of atoms and molecules to the interior of the cell. The principle model used to describe this process involves the opening of small (a few nm in radius) openings or pores. For this reason the process is referred to as electroporation although the term electropermeabilization is sometimes used. In this way previously administered drugs that ordinarily cannot pass through the membrane are able to enter the cell interior (electrochemotherapy, ECT) or DNA/RNA can be inserted into the cell nucleus (electrogenetherapy, EGT).

The applied field takes the form of square pulses with electric field amplitude, E, number, N, pulse duration, T, and pulse repetition rate, F. Typically, as any of these parameters increases, the probability of drug or DNA insertion increases, but so does the probability of cell damage. There is, thus, a trade-off between insertion success and cell survival. Typically, E is on the order of 10 kV/m to 100 kV/m and T is on the order of milliseconds to microseconds. Currently, nanosecond pulses with E on the order of 1 MV/m are being investigated for potential clinical applications. Below a certain threshold that depends on cell properties (e.g., type, radius, location in tissue, etc.) electroporation does not occur. For millisecond to microsecond pulses reversible electroporation begins above about 10 kV/m. Under these conditions transport to the cell interior occurs and the cell survives the process. At higher fields too much damage occurs and the cells do not survive. There are two categories of this irreversible electroporation. Cells can die because the membrane is so severely damaged that it does not reseal adequately. In such non-thermal irreversible electroporation (NTIRE) the target cells can be destroyed without damaging the surrounding veins and extracellular matrix [8]. At higher fields the cells and some of their surroundings are destroyed by heating.

Electroporation works by changing the potential difference across the membrane. As noted above, applied fields on the order of 10 to 100 kV/m can produce TMVi comparable to or greater than TMVo. Because the exterior cell surface is positive relative to the interior, TMVt will be greatest at the end of the cell facing the positive electrode (anode). At the opposite end

facing the negative electrode (cathode), TMVo essentially subtracts from TMVi so that TMVt is large, but somewhat smaller than at the positive end. Eq. (2) above is useful in understanding parameters affecting ordinary electroporation. For pulses in the microsecond to millisecond range $t >> \tau$ so that the term in parentheses reduces simply to 1. At the midline where $\cos \Theta = 0$, TMVt = TMVo. Because the greatest TMVts are at the two ends, those are the places where maximum insertion is ordinarily expected. Minimum insertion is expected at the midline. As E increases, insertion will occur at places further and further from the poles. To achieve a particular TMVi, larger fields are required for smaller cells. Once the pore has opened, the molecules in the surrounding fluid pass through it to the cell interior. Larger molecules require longer pulse durations to widen the pores and to maintain the electrical driving force for a longer period of time. The area of the cell surface permeabilized depends on E whereas the level of permeability of the surface depends on the number and duration of the pulses.

A currently unresolved problem in electroporation theory is that the cell membrane does not completely reseal itself after the removal of the field. Electroporated simple lipid membranes reseal themselves on a time scale of microseconds whereas cell membranes remain partially permeabilized for time scales on the order of minutes. Two models have been proposed for the delay in complete resealing [32]. Both involve lipids, one of the major constituents of the cell membrane. One involves a change in the conformation of the lipids that results in a metastable membrane structure that requires considerable time to decay. The other is the oxidation of the lipids which changes a variety of the membrane properties.

4.2. Clinical applications of electroporation

Important anti-cancer drugs such as cisplatin and bleomycin cannot easily cross the cell membrane. Application of electroporation pulses opens pores in the membrane through which the drugs can pass. Because drug insertion into the cell is now more efficient, the dose given to the patient can be reduced significantly and have fewer side effects. ECT is being used at numerous centers in Europe for a wide variety of tumors [8]. For deep-seated tumors NTIRE is used to destroy the cancer cells while preserving the surrounding tissue. Deep-seated tumors require complex procedures. Typically an MRI is used to provide a detailed mapping of the tissue types surrounding the tumor. Knowledge of the dielectric properties of the various tissue types permits the calculation of the field that would be applied at the tumor site for various possible electrode placements. Once the optimum electrode placement has been decided the MRI can be used to guide the surgeon's placement of the electrodes [33].

The administration of drugs through skin patches (transdermal drug delivery) requires that the drugs successfully pass through the skin to the tissue below. Such passage is typically blocked by the stratum corneum, which is the outermost layer of the skin. The stratum corneum is an approximately 15 μm thick, dry layer of dead cells. Just as this layer protects the body by restricting the loss of fluids from the body to the surroundings, it also prevents the passage of fluids from the surface to the interior. In traditional electrically-assisted drug delivery systems (iontophoresis) electrodes are placed on the surface and a field is applied. Two factors are involved in the assisted drug transport [34]. First, the electric field will push positively-charged drugs from the anode through the skin to the cathode. Negatively-charged

drugs are pushed from the cathode. Second, the charged ions pull some of the fluid along with them (electro-osmosis) and thus enhance the transport. Neutral drug molecules can be transported by this method.

Electroporation can offer an improved method of transdermal drug delivery [8]. Because the stratum corneum has a much greater electrical resistance than the lower skin layers, the electric field of the applied pulses is concentrated in it. The pulses increase its permeability to the drugs by opening pathways through it. In addition the field can apply a strong electrophoretic force to charged drug molecules to push them through the stratum corneum.

Because DNA is significantly larger than the anti-cancer drugs, it is more difficult to insert into the cell. The DNA is inserted in the form of plasmids, which are small, often circular segments that contain genetic information. Moreover, DNA is negatively charged as is the outer cell surface so that a natural repulsion of DNA from the membrane occurs. For these reasons two pulses are used to insert DNA (or RNA) into a cell. In the first stage a typical short, high voltage pulse is applied in order to open pores. In the second stage a lower voltage pulse is applied for a longer time to drive the negatively charged DNA plasmid into the cell membrane. This electrophoretic push will be effective only at the side of the cell facing the negative electrode. Use of bipolar pulses allows the entry of the DNA into both sides of the cell. At the end of the pulses the electric field part of the process is over with the DNA still in the membrane. At this point a process called endocytosis occurs in which the cell forms a vesicle around the plasmid and then draws it into the cell interior. The plasmid does not then passively diffuse into the cell nucleus but is actively transported by intracellular mechanisms. The endocytosis and active transport processes require hours after the end of the pulse for the plasmid to enter the nucleus and be expressed. The details of these processes are not well understood [9].

EGT is used clinically for vaccination or cancer treatment [9]. In typical vaccinations a molecule (antigen) is injected into muscle to produce a specific immune response by the body. In EGT vaccinations a plasmid that encodes the antigen is injected. Cell nuclei incorporate the plasmid and then produce the antigens that provoke the immune response. Clinical trials have been successfully carried out for conditions such as HIV and hepatitis B and C viruses. For cancer treatment the plasmids are injected into the tumors. Several strategies for the gene expression can be used to produce products that promote, for example, the stimulation of cell suicide, the activation of an immune response, or the suppression of blood vessel growth. EGT can be combined with ECT to provide a two-stage attack on the tumors.

4.3. Nanoporation

Recall from Section 3 that for times much less that the membrane time constant, τ, the electric field penetrates the cell interior. It may then be possible to porate the cell nucleus and other subcellular structures. Because the size of those structures is much smaller than the cell itself, according to Eq. (2) correspondingly larger electric fields must be applied to do so. In nanoporation electric fields on the order of 1–10 MV/m are applied for times on the order of nanoseconds (ns). The actual pulse duration is important in determining where the nanopulses have their greatest effect. According to Eq. (2) with $\tau \sim 1$ μs, pulse durations of 10 ns or less

will produce negligible changes in TMVi. Thus, the electric field is large in the cell interior and can porate interior structures. Conversely, pulse durations greater than 100 ns will produce a large membrane polarization and a reduced internal field. The application of very short pulses and their analyses are complicated so that reproducible results using such pulses are difficult to achieve. Pulses with duration in the range 11 to 100 ns are the most effective in producing reproducible results in the cell interior such as apoptosis (cell suicide) and release of calcium from intracellular stores [35].

5. Mechanisms and experiments

We present here an abbreviated description of the research we have conducted [36, 37] to determine the mechanism by which cells initially detect physiological strength electric fields. Identifying and understanding this mechanism is important for further developing the various applications described above. We also present an abbreviated description of some experiments that support this identification.

5.1. How cells detect electric fields

As described above, DC and low-frequency electric fields produce a wide variety of biological effects at the cellular and tissue levels. Although the emphasis here is on cell migration, wound healing and neural stimulation, electric fields produce a wide variety of other effects on cells as described in the CRC review [1]. Once a cell initially detects the field that information is transmitted throughout the cell to produce a wide variety of biochemical effects. A major question is—what is the initial transduction mechanism by which the cell detects the field?

As noted above, for DC fields and AC frequencies below about 1 MHz, applied electric fields cannot penetrate the plasma membrane because there is sufficient time for charge redistribution in the cytoplasm to essentially cancel the applied field. For DC fields, then, the initial transduction must take place at the plasma membrane or just beyond it. The transduction process must also transmit this information to the cell interior. Three mechanisms have been proposed for this initial transduction process: (1) electrodiffusion/osmosis [38, 39], (2) opening of voltage-gated channels [40], and (3) electromechanical torque exerted on the glycocalyx [41]. The electrodiffusion/osmosis model requires fields that are stronger than typical physiological strength fields applied for relatively long time intervals, and the changes in transmembrane potential produced by such fields are insufficient to open voltage-gated channels [37].

The fundamental principle of the electromechanical model is that electric fields and fluid shear forces share a common transduction mechanism—the production of torques on transmembrane glycoproteins. In the fluid force model [42] fluid shears on the glycocalyx core are transmitted to the cytoskeleton as forces that are then communicated as

http://dx.doi.org/10.5772/intechopen.71683

mechanical signals throughout the cell interior to activate biochemical signaling pathways. The glycocalyx is the carbohydrate rich zone on the cell surface [43]. It covers the surface of all eukaryotic cells, including cancer and stem cells [44]. Many of the glycoproteins comprising the glycocalyx are negatively charged, particularly those containing sialic acid [45]. Moreover, when placed in an electric field applied parallel to the cell surface, the negatively-charged glycocalyx experiences an electrical force tangential to the surface, analogous to that applied by a fluid shear. We applied this concept to the structural model of Weinbaum et al. [42] in which forces exerted on the glycocalyx brush structure are transmitted to the cytoskeleton and thus throughout the cell. Specifically, these forces produce an electromechanical torque about the cytoskeletal junction point and, thus, a force on the cytoskeleton itself [41, 46]. The magnitude of this cytoskeletal force is comparable to those of mechanical forces known to produce physiological effects [41]. A more complete description of this model is provided below.

The predictions of the electromechanical model are consistent with the galvanotaxis of keratinocytes [36] and amoeba [37]. Galvanotaxis serves as a convenient effect for comparing the three proposed mechanisms because it is a process that is readily reproduced and is easily measured in real time. One can record the effect of the field as it occurs rather than wait for the results of a biochemical analysis. The same initial transduction process should be present for a variety of other field effects. The model successfully predicted that the superposition of a 40 V/m, 1.6 Hz sinusoidal signal on a 100 V/m DC field would reduce directionality whereas the superposition of a 40 V/m, 160 Hz field would not reduce directionality compared to a pure 100 V/m DC field. Further confirmation of the electromechanical model, which identifies the glycocalyx as the transduction site, has been provided by Finkelstein et al. [47] who showed that removal of the major negatively charged molecules in the glycocalyx in 3 T3 and HeLa cells eliminated galvanotaxis. Moreover, the effect of the superimposed fields on cell motility (speed) is also explained by the model [37]. An increase in cell motility often, but not always, accompanies the increase in directionality toward the field. The applied field produces a bending torque on the negatively-charged glycocalyx between the cell and the substrate. The glycocalyx is bent away from the substrate, increasing the glycocalyx-substrate separation and increasing cell adhesion. As a result, cell motility can increase. However, if the cell adhesion is already optimal, the field does not produce a significant additional motility increase. The addition of positively-charged calcium ions that bind to the negatively-charged glycocalyx reduced the increase in directionality and motility produced by the field on amoeba—providing further confirmation of the electromechanical model [37]. The details are presented below.

Because similar behavior is exhibited by such different cell types, we surmise that this field-detection mechanism must have been present in early cells. We suggest [37] that this glycocalyx-bending mechanism was initially used to detect fluid flow changes. Because that detection system happened to be negatively charged, it could also detect electric fields. With the evolution of multicellular organisms, this ability might have become useful in controlling some developmental processes [4]. Other field sensing processes then followed.

5.2. Details of the mechanical model

5.2.1. Directionality increase

The first mechanism by which an electric field is detected by a cell involves the production of an electromechanical torque on the glycocalyx by the field that is analogous to the torque produced by fluid shear. Although a glycocalyx covers the surface of all eukaryotic cells [44], detailed modeling of its functionality has been carried out primarily for endothelial cells. For this reason the parameters used in the modeling rely on parameters for the glycocalyx of endothelial cells and their components. In their review of the structure of the endothelial glycocalyx, Curry and Adamson [48] describe an inner layer with a thickness of 100–150 nm that possesses a quasi-periodic structure. Beyond that layer there is a region out to 400 nm that is required for fluid shear detection. The fluid shear stress applied toward the top of that region is transmitted to the more rigid inner layer and then transferred to the membrane as a solid mechanical force [44].

Figure 4 illustrates the basic electromechanical model [36]. It shows the forces acting on a charged, cylindrical glycoprotein that is connected at its base to the cytoskeleton. $F_{elec} = QE(t)$ is the electrical force exerted on the effective charge, Q, of the glycoprotein by the applied electric field, E(t), at time t. Because the glycocalyx is negatively charged, the force, F, exerted on it by the field, E, is opposite in direction to E. $F_{drag} = -cd\theta(t)/dt$ is the viscous force exerted on the rod by the surrounding extracellular fluid. The angular displacement of the rod, θ (t), is determined by torque balance [46] and c is the frictional drag coefficient. For a rod $c = 2\pi L'^2/$

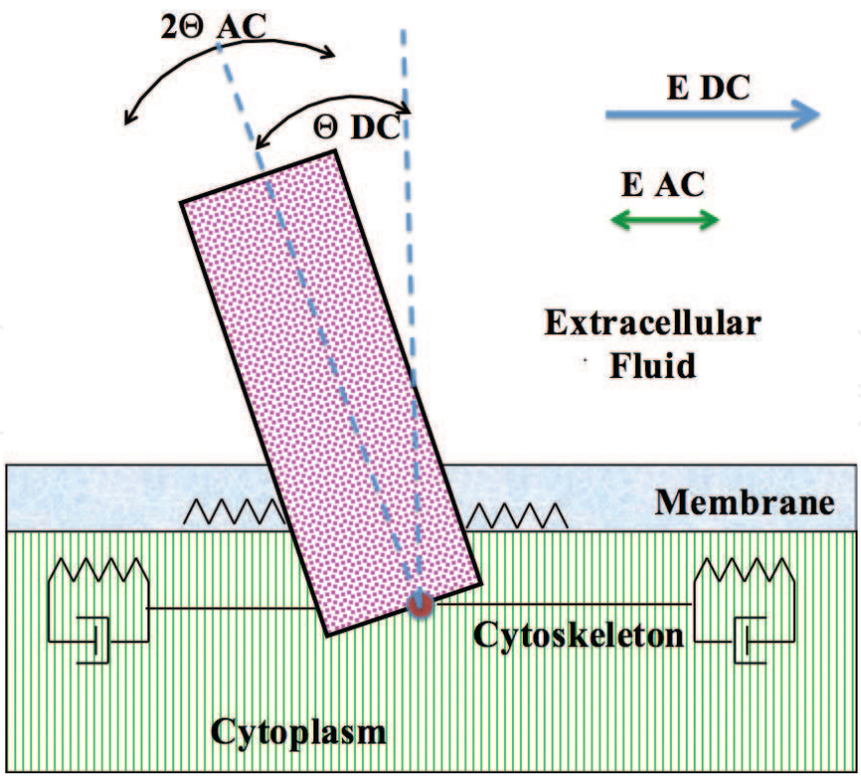

Figure 4. Schematic diagram of the forces acting on a glycocalyx rod under the application of an electric field.

(ln[L′/r] − 0.447) where L′ is the length of the rod and r is its radius [41]. $F_{memb} = -kh\theta(t)$ is the harmonic restoring force exerted on the oscillating rod by the cell membrane where k is the force constant and h is the distance from the center of the membrane to the base connection point with the cytoskeleton [41]. F_{base} is the force exerted by the cytoskeleton on the rod at the connection point. According to Newton's Third Law, the force exerted on the cytoskeleton by the rod is $-F_{base}$. Newton's Second Law states the net force, F_{net}, acting on the rod is

$$F_{net} = Ma = F_{elec} + F_{drag} + F_{memb} + F_{base} \quad (3)$$

where M is the mass of the rod and a is the acceleration of its center of mass. Here $a = (L'/2)\, d^2\theta/dt^2$. Solving, one has

$$F_{base} = (ML/2)\, d^2\theta(t)/dt^2 - QE(t) + cd\theta(t)/dt + kh\theta(t) \quad (4)$$

The spring/dashpot combinations connected to the base in **Figure 4** indicate the transmission of the resulting longitudinal mechanical signals along the cytoskeleton to the rest of the cell. The angular displacement illustrates the situation in which the applied field has both DC and AC components. For a purely DC field θ AC and E AC are zero.

Application of the above model to the array of 27 glycocalyx rods in Weinbaum's glycocalyx model [42] yields a force applied to the cytoskeleton on the order of 0.5 pN for an applied electric field of 100 V/m. Such a force is comparable to some intracellular mechanical forces [41]. Hence, it is plausible that forces predicted by the electromechanical model would have physiological effects.

The viscous drag force exerted on the rod by the surrounding extracellular fluid increases linearly with the frequency of the applied field. The importance of this frequency dependence becomes apparent when the AC field is superimposed on a pure DC field. The drag exerted on the rods for the 1.6 Hz field is very small so that the total force (AC + DC) on the cytoskeleton is strongly modulated. The drag force for the 160 Hz field is 100 times larger so that the resulting modulation is negligible, and the total force is essentially identical to that produced by a pure DC field [41]. We suggest that the strong modulation at 1.6 Hz introduces significant mechanical signaling noise in the cytoskeleton that reduces the overall transduction relative to a pure DC field. No such reduction would be produced by the superimposed 160 Hz field. The electromechanical model is thus consistent with the results presented for keratinocytes [36] and for amoeba [37].

5.2.2. Motility increase

The mechanism described above cannot explain the increase in speed produced by the applied fields, DC and/or AC. Cell motility is determined in part by the adhesion of the cell to the substrate [49]. Cells that are either too tightly or too loosely bound will have lower motility than those with an intermediate adhesion. The adhesion is reduced by the negatively charged glycocalyx [50, 51]. Increasing the distance between the glycocalyx and the substrate should then increase adhesion and increase motility.

The model described above, regarding directionality involves the interaction of the field with the relatively rigid inner glycocalyx. The model described here, regarding motility increase, involves the interaction with the relatively flexible outer glycocalyx. Recent measurements have shown that the entire glycocalyx for endothelial cells may extend out to 11,000 nm with a loose fibril mesh of elongated elements [52].

Amoeba have a negatively-charged glycocalyx [53], the full extent of which is not well known. Electron micrographs by Topf and Stockem [54] showed that the glycocalyx consists of a compact base layer that is approximately 70 nm thick with an outer, filamentous layer that is approximately 400 nm thick. As noted above, recent advances in microscopic techniques indicate that a typical glycocalyx thickness is on the order of several thousand nanometers or more. Grebecki et al. [55] showed that *Amoeba proteus* adheres to the substrate using discretely-spaced "minipodia" that are about 500 nm thick and up to 8000 nm long. Hence the outer glycocalyx between the amoeba's cell body and the substrate is not compressed but should be relatively free to reorient itself in an applied field.

Cruz-Chu et al. [56] used a molecular-dynamics simulation to investigate the effects of fluid shear on a model glycocalyx. They found that an applied shear of 0.47 MPa produced dramatic bending of the glycocalyx (cf. their Figure 5b). Stresses of about 3 MPa and greater significantly disrupted the glycocalyx. Although their model was applied primarily to the inner glycocalyx, similar bending should also be produced in the less rigid outer glycocalyx that interacts with the substrate.

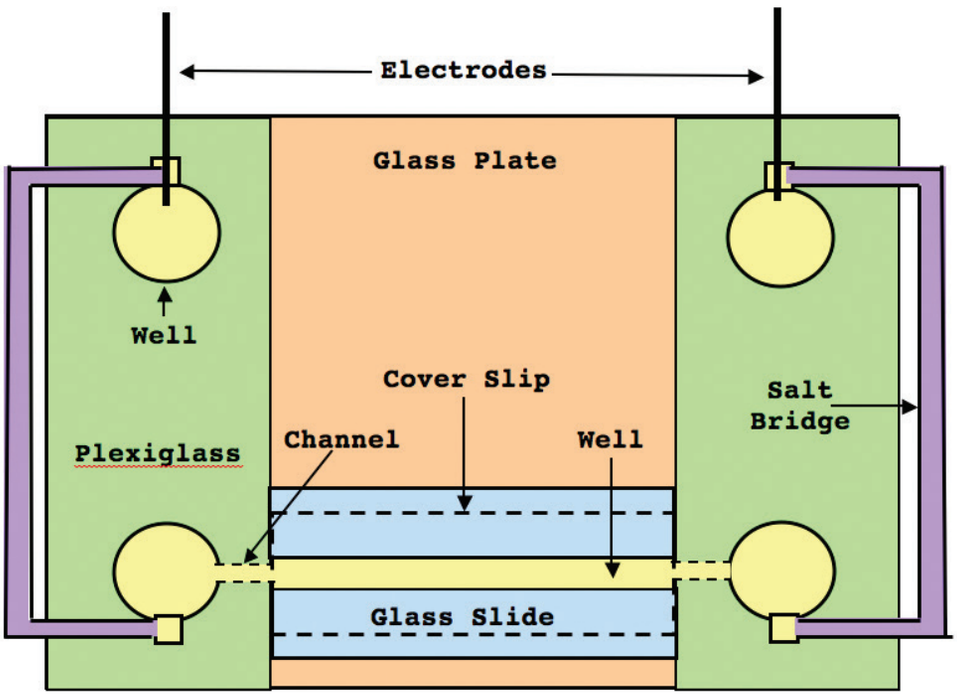

Figure 5. Schematic diagram of the system used to expose amoeba to an applied electric field.

We can estimate the tangential shear produced by a physiological strength electric field. For simplicity we model the amoeba glycocalyx as a uniform, negatively-charged, rectangular-solid gel that fills the space between the amoeba body and the substrate. We assume that the amoeba is already elongated in the direction of the field. The length, L, and width, W, of the rectangular solid are those of the amoeba which we take to be L = 0.2 mm and W = 0.05 mm. We take the thickness of the glycocalyx to be the length of the amoeba minipodia, T = 8 μm [55]. A typical estimate for the charge density of the glycocalyx is ρ = 25 mEq/l or 2.5×10^6 C/m^3 [57]. The electric force on this model glycocalyx is then F = ρLWTE. The shear stress, σ, is that force divided by the cross-section to which it is applied or

$$\sigma = \rho LWTE/WT = \rho LE \tag{5}$$

For an electric field of 200 V/m, σ is 0.1 MPa. Our calculated shear stress produced by the field should then be sufficient to bend the glycocalyx. Bending the glycocalyx increases its separation from the substrate. Increasing the separation increases the cell's adhesion and, thus, its motility.

The response to a shear stress depends on the mechanical properties of the glycocalyx. The shear stress modulus and the shear loss modulus of the glycocalyx increase with the frequency of the applied stress [58]. Consequently the bending produced by a 160 Hz electric field should be less than that produced by a 1.6 Hz field. As a result, the increase in motility should be less for a 160 Hz field that for a 1.6 Hz field, as reported in Ref. [37].

5.3. Galvanotaxis experimentation to validate the model

5.3.1. Experimental setup

Amoeba were purchased from Carolina Biological Company (Burlington, NC, USA), and cultured in the container in which they were shipped for at least 3 days before they were used in experiments. The details of the design and construction of the apparatus (**Figure 5**) used for all the experiments are found in Hart and Palisano [37]. Briefly, the amoeba cells were isolated from the wells containing the Pt wire source of current and placed in the trough that we connected to the wells to which the electrical current was introduced by salt bridges.

Because of the complex geometry it was necessary to model numerically the field inside the trough for a given voltage applied to the wells using COMSOL Multiphysics (COSMOL Inc., Burlington, MA, USA). COSMOL Multiphysics was also used to model the temperature increase of electric fields during the 40-minute time interval of experiments and indicated that the temperature increase produced was than 1°C. The field and temperature calculations were confirmed by measurements with a voltmeter and thermocouple probe, respectively.

In all experiments, each amoeba served as it owns control. During the first 20 minutes of recording, the movement of the amoeba cells occurred in the absence of an electric field. In the last 40 minutes an electric field was applied. Cell movements were recorded for the entire 60-minute experiment and snapshots were taken from the movie at 1-minute intervals and converted to a

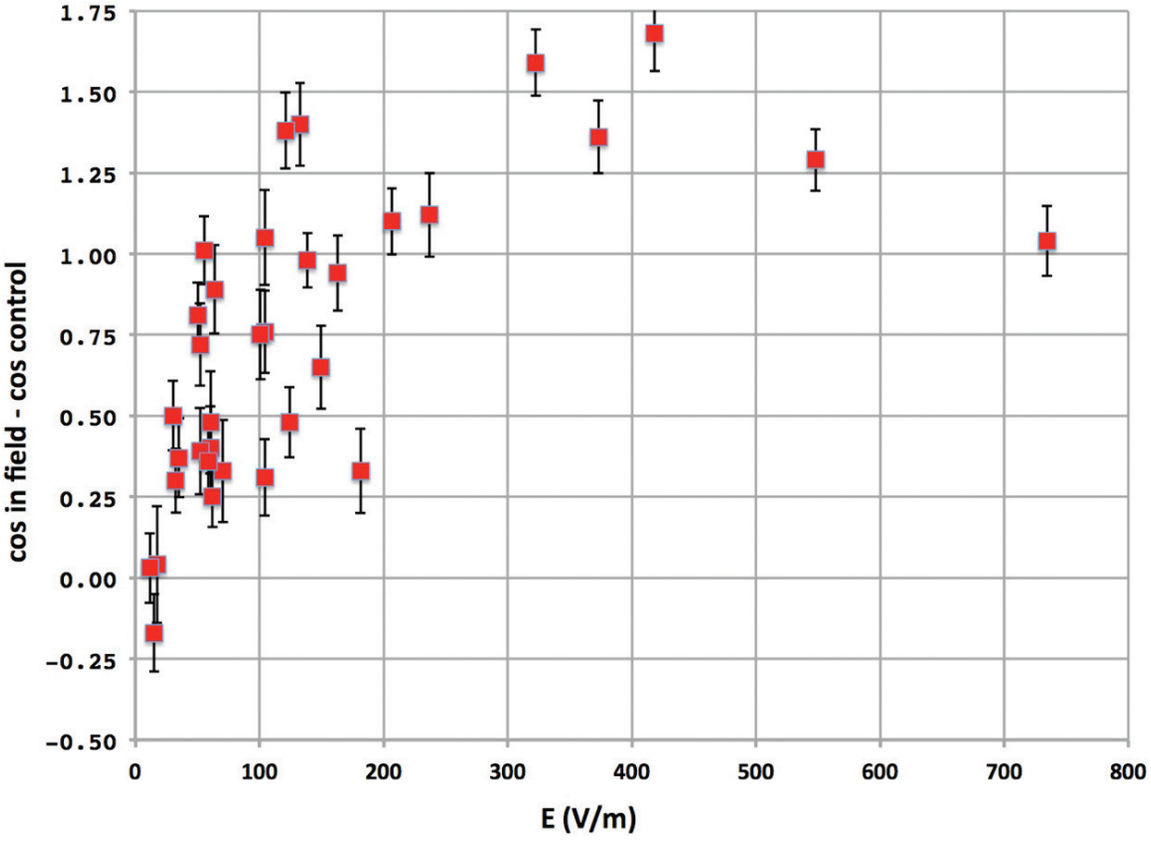

Figure 6. Increase in directionality in the DC field: Cosine during the last 10 minutes in the field minus the cosine during the last 10 minutes of control for each individual cell, averaged over all the cells. Error bars represent the standard error of the mean.

time-lapse movie. The positions of each amoeba at each 1-minute interval were digitized from the movie using LoggerPro (Venier Software & Technology, Beaverton, OR, USA) software.

5.3.2. Galvanotaxis results

We applied DC electric fields ranging from 15 V/m to 800 V/m. The number of cells tracked in an experiment typically ranged between 25 and 35. The position of each amoeba is tracked at 1-minute intervals during a 20-minute control period during which no field is applied and in the subsequent 40-minute interval during which a field is applied. During each 1-minute interval, an amoeba travels a distance, d. The sum of all these distances over a particular interval of time is the total distance traveled, D, during that interval. The average speed or motility of an individual amoeba in each interval is D/T where T is the duration of the interval, here 10 minutes. We consider the D/T ratio for the last 10 minutes of control as the control motility and that ratio for the final 10 minutes of the field as the final motility. The field is directed along the x-axis. During any 10-minute interval the distance traveled by an amoeba in the direction of the field is Δx. The orientation of the amoeba movement relative to the field is parameterized by angle Φ where $\cos \Phi = \Delta x/D$. We refer to $\cos \Phi$ as the "directionality" of the amoeba. A value of $\cos \Phi = +1$ indicates migration parallel to the field whereas −1

represents migration directly opposite the field. We consider the cosine for the last 10 minutes of control as the control directionality and the cosine for the final 10 minutes of the field as the field directionality.

Figure 6 compares the difference of the field and control directionalities of an individual cell, averaged over all the cells, as a function of the applied field. Hence, each cell serves as its own control. As evidenced by the increase in directionality, the cells begin to detect fields greater than about 30 V/m. The increase in directionality improves as the field increases and becomes relatively steady for fields above about 200 V/m. There is noticeable variation in the increases for low fields, but the overall trend is apparent. For weaker fields,

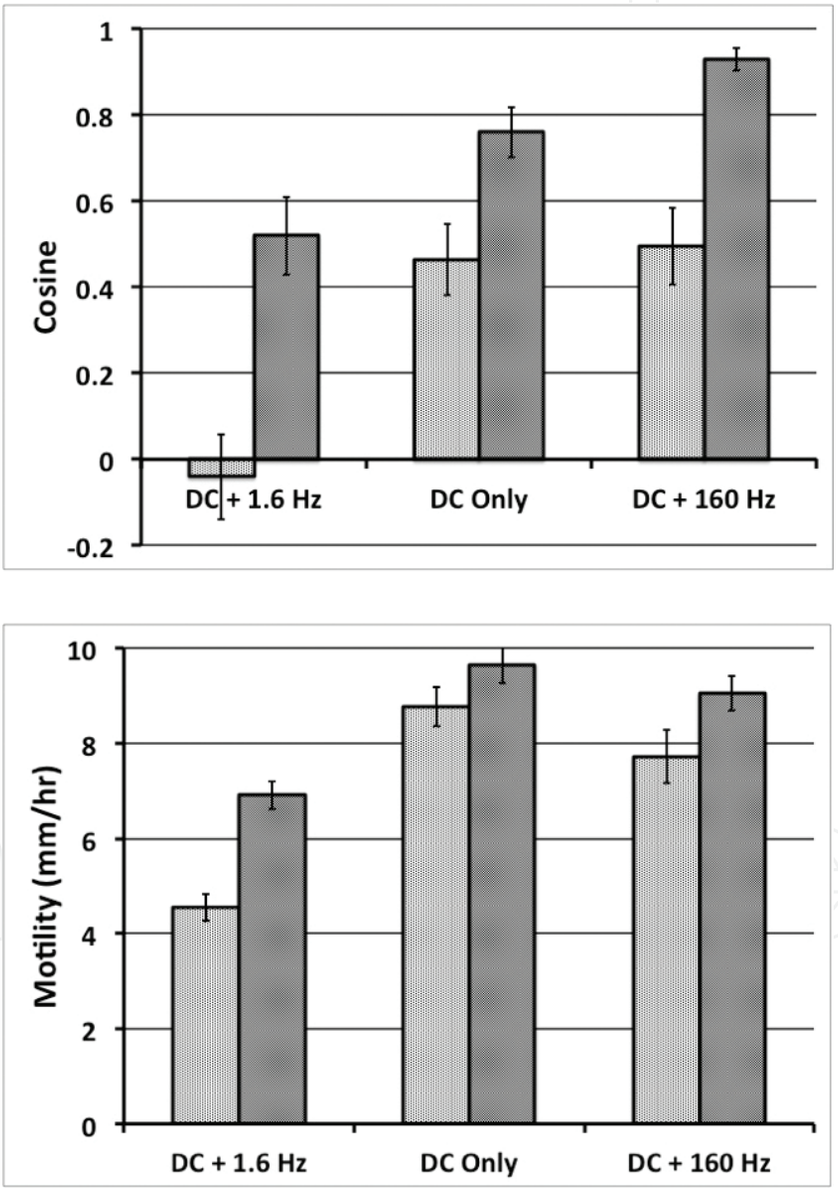

Figure 7. The effect on directionality and motility of superimposing a smaller AC field on a DC field. In each case the DC field was about 65 V/m and the AC field was about 32 V/m. The light shading indicates values obtained during the first 10 minutes the field was applied; the dark shading, the last 10 minutes. Error bars represent the standard error of the mean. (A) Illustrates the differences in directionality; (B) the differences in speed.

nearly 40 minutes are required to detect an increase in directionality. Thus, comparisons of directionality increase for different applied fields are made for the last 10 minutes of field application.

Measurement of cell motility indicated that cells with low control motility increased their speeds much more dramatically than did cells with a high initial motility [37]. A clear motility increase of about 50% began above about 60 V/m and improved out to about 200 V/m beyond which field there was considerable variability. The motility increase became smaller with greater control motility. There was no clear, corresponding variation of the directionality increase with control motility.

One of the goals of this research is to examine how widespread is the applicability of the electromechanical model. Hart et al. [36] demonstrated that it described well the loss of directionality of keratinocytes when a weaker, low-frequency AC field was superimposed on a stronger DC field. **Figure 7** indicates that a similar response was observed in *Amoeba proteus*, a free-living cell. The directionality and motility of amoeba were compared when exposed to a 65 V/m DC field alone, a 32 V/m, 1.6 Hz AC field superimposed on a 65 V/m DC field or a 32 V/m, 160 Hz AC field superimposed on a 65 V/m DC field. In each case the average electric field was 65 V/m DC. The three sets of cells all came from the same shipment and were thus exposed to similar conditions prior to the experiments.

Figure 7A shows that directionality is eliminated for the added 1.6 Hz field during the first 10 minutes, but is comparable and significant for the pure DC and added 160 Hz fields. The directionality is improved for all three cases during the final 10 minutes. Although greatly improved, the directionality for the added 1.6 Hz case is still less than the other two cases. These results are similar to those obtained for keratinocytes [36]. **Figure 7B** illustrates that the motility during the first 10 minutes for the added 1.6 Hz case is much lower than for the other applied fields. As with directionality, the motility for the added 1.6 Hz case has improved for the last 10 minutes, but is still less than the motilities of the other two cases. These results are consistent with the motility model described above.

6. Numerical simulations

The applicability of the methods described above requires knowledge of the detailed electric field distribution at the site of its application. Because the field distribution depends on the electrical properties and physical shapes of the various cells and tissues involved, numerical methods must be used for the calculation [59]. These methods have evolved considerably over the years. For example, spreadsheet cells can be used to represent small volume elements in a limb. The value of the cell is the electrical potential of the element, Vo. That value is related to the potential of the six surrounding cells in the three-dimensional model. Setting the current entering the cell equal to the current leaving relates Vo to the potentials of the surrounding cells via the inter-cell resistivities. The electrical anisotropies of the tissue can be introduced in this manner. The fundamental equations can be introduced into many similar cells simultaneously and solved by the method of successive over-relaxation in an Excel spreadsheet. This

approach was used to determine how the electric field at the site of a tibia fracture evolved as the injury healed during an electrical fracture-healing treatment [60]. The method can even be extended to calculate the electric field distribution induced in a complex distribution of cells in a culture dish [61].

More recently, commercial software programs are used to determine more precisely and rapidly the field distribution in complicated situations. As noted above in Section 5.3.1, COMSOL Multiphysics (COSMOL Inc., Burlington, MA, USA) was used to determine both the electric field and temperature distributions in our experimental setup. Electrode placement for the administration of electroporation pulses requires the detailed numerical analysis of the resulting fields at and surrounding the tumor site [8]. Full-body animal and human virtual models are now available for very detailed electric field computations [62]. The models contain information regarding the electrical, thermal and flow properties of the various tissues. In this way a comprehensive analysis of the field distribution and its associated physical effects can be determined for various electrode placements.

7. Conclusions

Electric fields have a wide variety of applications in biology and medicine. Physiological strength fields are used to improve the healing of wounds, the stimulation of neurons and the positioning and activation of cells on scaffolds for tissue engineering purposes. The brief, strong pulses used in electroporation are used to improve the insertion of drugs into tumors and DNA into cell nuclei. Numerical simulations must be used to select the proper field strengths to be applied in a clinical setting. Some fundamental issues are still being addressed; in particular, how do cells actually detect the fields? The electromechanical model described here is consistent with the experimental evidence whereas other models are not.

Author details

Francis X. Hart[1]* and John R. Palisano[2]

*Address all correspondence to: fhart@sewanee.edu

1 The Department of Physics, The University of the South, Sewanee, TN, USA

2 The Department of Biology, The University of the South, Sewanee, TN, USA

References

[1] Pullar CE, editor. The Physiology of Bioelectricity in Development, Tissue Regeneration, and Cancer. Boca Raton, FL: CRC Press; 2011. 342 p

[2] McCaig CD, Rajnicek AM, Song B, Zhao M. Controlling cell behavior electrically: Current views and future potential. Physiological Reviews. 2005;**85**:943-978. DOI: 10.1152/physrev.00020.2004

[3] Robinson KR, Messerli MA. Left/right, up/down: The role of endogenous electric fields as directional signals in development, repair and invasion. BioEssays. 2003;**25**:759-766. DOI: 10.1002/bies.10307

[4] Levin M. Molecular bioelectricity: How endogenous voltage potentials control cell behavior and instruct pattern regulation in vivo. Molecular Biology of the Cell. 2014;**25**:3835-3850. DOI: 10.1091/mbc.E13-12-0708

[5] Meng S, Rouabhia M, Zhang Z. Electrical stimulation modulates osteoblast proliferation and bone protein production through heparin-bioactivated conductive scaffolds. Bioelectromagnetics. 2013;**34**:189-199. DOI: 10.1002/bem.21766

[6] Hart FX. Bioimpedance in the clinic. Zdravstveni Vestnik. 2009;**78**:782-790

[7] Pullar CE, Isseroff RR. Cyclic AMP mediates keratinocyte directional migration in an electric field. Journal of Cell Science. 2005;**118**:2023-2034. DOI: 10.1242/jcs.02330

[8] Yarmush ML, Golberg A, Sersa G, Kotnik T, Miklavic D. Electroporation-based technologies for medicine: Principles, applications and challenges. Annual Review of Biomedical Engineering. 2014;**16**:295-320. DOI: 10.1146/annurev-bioeng-071813-104622

[9] Rosazza C, Meglic SH, Zumbusch A, Rols M-P, Miklavcic D. Gene electrotransfer: A mechanistic perspective. Current Gene Therapy. 2016;**16**:98-129

[10] Pullar CE, Isseroff RR, Nuccitelli R. Cyclic AMP-dependent protein kinase a plays a role in directed migration of human keratinocytes in a dc electric field. Cell Motility and the Cytoskeleton. 2001;**50**:207-217

[11] Nuccitelli R. A role for endogenous electric fields in wound healing. Current Topics in Developmental Biology. 2003;**58**:1-26

[12] Kloth LC. Electrical stimulation technologies for wound healing. Advances in Wound Healing. 2014;**3**:81-90. DOI: 10.1089/wound.2013.0459

[13] Pullar CE. The biological basis for electric stimulation as a therapy to heal chronic wounds. Journal of Wound Technology. 2009;**N6**:20-24

[14] Hoare JJ, Rajnicek AM, McCaig CD, Barker RN, Wilson HM. Electric fields are novel determinants of human macrophage functions. Journal of Leukocyte Biology. 2016;**99**:1141-1151. DOI: 10.1189/jlb.3A0815-390R

[15] The Parkinson Foundation. Deep Brain Stimulation http://www.parkinson.org/understanding-parkinsons/treatment/surgery-treatment-options/Deep-Brain-Stimulation

[16] Ho CH et al. Functional electrical stimulation and spinal cord injury. Physical Medicine and Rehabilitation Clinics of North America. 2014;**25**:631-ix. DOI: 10.10.1016/j.pmr.2014.05.001

[17] Rejc A, Angeli C, Harkema S. Effects of lumbosacral spinal cord epidural stimulation for standing after chronic complete paralysis in humans. PLoS ONE; **10**(7): e0133998. https://doi.org/10.1371/journal.pone.0133998

[18] Solopova IA, Sukhotina IA, Zhvansky DS, Ikoeba GA, Vissarionov SV, Baindurashvili AG, Edgerton VR, Gerasimenko YP, Moshonkina TR. Effects of spinal cord stimulation on motor functions in children with cerebral palsy. Neuroscience Letters. 2017;**639**:192-198. DOI: 10.1016/j.neulet.2017.01.003

[19] DeSantana JM, Walsh DM, Vance C, Rakel BA, Sluka KA. Effectiveness of transcutaneous electrical nerve stimulation for treatment of hyperalgesia and pain. Current Rheumatology Reports. 2008;**10**:492-499

[20] Hart FX, Evely K, Finch C. The use of a spreadsheet program to calculate the electric field/current distributions induced in irregularly-shaped inhomogeneous biological structures by low-frequency magnetic fields. Bioelectromagnetics. 1993;**14**:161-172

[21] Griffin M, Bayat A. Electrical stimulation in bone healing: Critical analysis by evaluating levels of evidence. Eplasty. 2011;**11**:303-353

[22] Aleem IS, Aleem I, Evaniew N, Busse JW, Yaszemski M, Agarwal A, Einhorn T, Bhandari M. Efficacy of electrical stimulators for bone healing: A meta-analysis of randomized sham-controlled trials. Scientific Reports. 2016;**6**:31724. DOI: 10.1038/srep31724

[23] Ueno S, Sekino M. Biomagnetics: Principles and Applications of Biomagnetic Stimulation and Imaging. Boca Raton, FL: CRC Press; 2017. 342 pp

[24] Miklavcic D, Pavselj N, Hart FX. Electric properties of tissues. In: Akay M, editor. Wiley Encyclopedia of Biomedical Engineering. Vol. 6. New York: Wiley. 2006. p. 3578-3589

[25] Radisic M, Park H, Shing H, Consi T, Schoen FJ, Langer R, Freed LE, Vunjak-Novakovic G. Functional assembly of engineered myocardium by electrical stimulation of cardiac myocytes cultured on scaffolds. PNAS. 2004;**101**:18129-18134. www.pnas.org/cgi. DOI: 10.1073/pnas.0407817101

[26] Weng B, Liu X, Shepherd R, Wallace GG. Inkjet printed polypyrrole/collagen scaffold: A combination of spatial control and electrical stimulation of PC12 cells. Synthetic Metals. 2012;**162**:1375-1380. DOI: 10.1016/j.synnthmet.2012.05.022

[27] Bodhak S, Bose S, Kinsel WC, Bandyopadhyay A. Investigation of *in vitro* bone cell adhesion and proliferation on Ti using direct current stimulation. Materials Science and Engineering. 2012;**C32**:2163-2168. DOI: 10.1016/j.msec.2012.05.032

[28] Hoi Ting HA, Cheng I, Chowdhury MF, Radisic M. Interactive effects of surface topography and pulsatile electrical field stimulation on orientation and elongation of fibroblasts and cardiomyocytes. Biomaterials. 2007;**28**:4277-4293. DOI: 10.1016/j.biomaterials.2007.06.001

[29] Rajnicek AM, Foubister LE, McCaig CD. Alignment of corneal and lens epithelial cells by co-operative effects of substratum topography and DC electric fields. Biomaterials. 2008;**29**:2082-2095. DOI: 10.1016/j.biomaterials.2008.01.015

[30] Arinzeh TL, May J, Huang GP. Structural support for damaged tissue repair. American Scientist. 2017;**105**:298-305

[31] Hronik-Tupaj M, Kaplan DL. A review of the responses of two and three-dimensional engineered tissues to electric fields. Tissue Engineering: Part B. 2012;**18**:167-180. DOI: 10.1089/ten.teb.2011.0244

[32] Rems L, Miklavcic D. Tutorial: Electroporation of cells in complex materials and tissue. Journal of Applied Physics. 2016;**119**:201101-1-21. DOI: 10.1063/1.4949264

[33] Miklavcic D, Davalos RV. Electrochemotherapy (ECT) and irreversible electroporation (IRE)–Advanced techniques for treating deep-seated tumors based on electroporation. BioMedical Engineering Online. 2015;**14**(Suppl 3):I1

[34] Roustit M, Blaise S, Cracowski J-L. Trials and tribulations of skin iontophoresis in therapeutics. British Journal of Clinical Pharmacology. 2013;**77**:63-71. DOI: 10.1111/bcp.12128

[35] Napotnik TB, Rebersek M, Vernier PT, Mali B, Miklavcic D. Effects of high voltage nanosecond electric pulses on eukaryotic cells (*in vitro*): A systematic review. Bioelectrochemistry. 2016;**110**:1-12. DOI: 10.1016/j.bioelectrochem.2016.02.011

[36] Hart FX, Laird M, Riding A, Pullar CE. Keratinocyte galvanotaxis in combined DC and AC electric fields supports an electromechanical transduction sensing mechanism. Bioelectromagnetics. 2013;**34**:85-94. DOI: 10.1002/bem.21748

[37] Hart FX, Palisano JR. Glycocalyx bending by an electric field increases cell motility. Bioelectromagnetics. 2017;**38**:482-493. DOI: 10.1002/bem.22060

[38] Jaffe LF, Nuccitelli R. Electrical controls of development. Annual Review of Biophysics and Bioengineering. 1977;**6**:445-476

[39] McLaughlin S, Poo M-M. The role of electro-osmosis in the electric-field-induced movement of charged macromolecules on the surface of cells. Biophysical Journal. 1981; **34**:85-93

[40] Djamgoz MB, Mycielska M, Madeja Z, Fraser SP, Korohoda W. Directional movement of rat prostate cancer cells in direct-current electric field: Involvement of voltage-gated Na+ channel activity. Journal of Cell Science. 2001;**114**:2697-2705

[41] Hart FX. Cytoskeletal forces produced by extremely low-frequency electric fields acting on extracellular glycoproteins. Bioelectromagnetics. 2010;**31**:77-84. DOI: 10.1002/bem.20525

[42] Weinbaum S, Zhang X, Han Y, Vink H, Cowin SC. Mechanotransduction and flow across the endothelial glycocalyx. Proceedings of the National Academy of Sciences. 2003;**100**:7988-7995 www.pnas.org/cgi/doi/10.1073/pnas.1332808100

[43] Alberts B, Johnson A, Lewis J, Raff M, Roberts K, Walter P. Molecular Biology of the Cell. 6th ed. New York: Garland Press; 2015. p. 582

[44] Tarbell JM, Shi Z-D. Effect of the glycocalyx layer on transmission of interstitial flow shear stress to embedded cells. Biomechanics and Modeling in Mechanobiology. 2013; **12**:111-121. DOI: 10.1007/s10237-012-0385-8

[45] Barker AL, Konopatskaya O, Neal CR, Macpherson JV, Whatmore JL, Winlove CP, Unwin PR, Shore AC. Observation and characterization of the glycocalyx of viable human endothelial cells using confocal laser scanning microscopy. Physical Chemistry Chemical Physics. 2004;**6**:1006-1011. DOI: 10.1039/b312189e

[46] Hart FX. The mechanical transduction of physiological strength electric fields. Bioelectromagnetics. 2008;**29**:447-455. DOI: 10.1002/bem.20411

[47] Finkelstein EI, Chao PG, Hung CT, Bulinski JC. Electric field-induced polarization of charged cell surface proteins does not determine the direction of galvanotaxis. Cell Motility and the Cytoskeleton. 2007;**64**:833-846. DOI: 10.1002/cm.20227

[48] Curry FE, Adamson RH. Endothelial glycocalyx: Permeability barrier and mechanosensor. Annals of Biomedical Engineering. 2012;**40**:828-839. DOI: 10.1007/s10439-011-0429-8

[49] Barnhart EL, Lee K-C, Keren K, Mogliner A, Theriot JA. An adhesion-dependent switch between mechanisms that determines motile cell shape. PLoS Biology. 2011;**9**:e1001059. DOI: 10.1371/journal.pbio.1001059

[50] Kolodziejczyk J, Klopocka WK, Lopatowska A, Grebecka L, Grebecki A. Resumption of locomotion by *Amoeba proteus* readhering to different substrata. Protoplasma. 1995; **189**:180-186

[51] Sabri S, Soler M, Foa C, Pierres A, Benoliel A-M, Bongrand P. Glycocalyx modulation is a physiological means of regulating cell adhesion. Journal of Cell Science. 2000; **11**:1589-1600

[52] Ebong EE, Macaluso FP, Spray DC, Tarbell JM. Imaging the endothelial glycocalyx in vitro by rapid freezing/freeze substitution transmission electron microscopy. Arteriosclerosis, Thrombosis, and Vascular Biology. 2011;**31**:1908-1915. DOI: 10.1161/ATVBAHA.111.225268

[53] Brewer JE, Bell LGE. Long-range electrostatic interactions between amoebae and anion-exchange particles. Experimental Cell Research. 1970;**61**:397-402

[54] Topf P-M, Stockem W. Protein and lipid composition of the cell surface complex from *Amoeba proteus* (Rhizopoda: Amoebida). European Journal of Protistology. 1996; **32**:156-170

[55] Grebecki A, Grebecka L, Wasik A. Minipodia, the adhesive structures active in locomotion and endocytosis of amoebae. Acta Protozoologica. 2001;**40**:235-247

[56] Cruz-Chu ER, Malafeev A, Pajarskas T, Pivkin IV, Koumoutsakos P. Structure and response to flow of the glycocalyx layer. Biophysical Journal. 2014;**106**:232-243. DOI: 10.1016/j.bpj.2013.09.060

[57] Chen B, Fu BM. An electrodiffusion-filtration model for effects of endothelial surface glycocalyx on microvessel permeability to macromolecules. Journal of Biomechanical Engineering. 2004;**126**:614-624. DOI: 10.1115/1.1800571

[58] Nijenhuis N, Mizuno D, Spaan JAE, Schmidt CF. Viscoelastic response of a model endothelial glycocalyx. Physical Biology. 2009;**6**:1-8. DOI: 10.1088/1478-3975/6/2/025014

[59] Hart FX. Investigation systems to study the biological effects of weak physiological electric fields. In: Pullar C, editor. The Physiology of Bioelectricity in Development, Tissue Regeneration and Cancer. Boca Raton, FL: CRC Press; 2011. pp. 17-38

[60] Hart FX. Changes in the electric field distribution at an injury site during healing under electrical stimulation. Journal of Bioelectricity. 1991;**10**:33-51

[61] Hart FX. Cell culture dosimetry for low frequency magnetic fields. Bioelectromagnetics. 1996;**17**:48-57

[62] IT^{IS} Foundation. EM Research. Virtual Population. https://www.itis.ethz.ch/virtual-population/